Available online at www.sciencedirect.com

ScienceDirect

Procedia Engineering 130 (2015) 135 – 149

Procedia Engineering

www.elsevier.com/locate/procedia

14th International Conference on Pressure Vessel Technology

Uncertainty Quantification of Stresses in a Cracked Pipe Elbow Weldment Using a Logistic Function Fit, a Nonlinear Least Square Algorithm, and a Super-Parametric Method[1]

J.T. Fong[a,*], J.J. Filliben[a], N.A. Heckert[a], P.V. Marcal[b], R. Rainsberger[c], L. Ma[a]

[a]*U. S. National Institute of Standards & Technology, Gaithersburg, MD 20899, U.S.A.*
[b]*MPACT Corp., 5297 Oak Bend Lne., Oak Park, CA 91377, U.S.A.*
[c]*XYZ Scientific Applications, Inc., 2255 Morello Ave., Suite 220., Pleasant Hill, CA 94523, U.S.A.*

Abstract

In a 3-part series of papers, of which this paper is Part II, we investigate the applicability of the fully quadratic hexa-27 element (see Part I) to four problems of interest to the pressure vessels and piping community: (1) The solid-element-based analysis of a welded pipe elbow with a longitudinal surface crack in one of its weldments. (2) The solid-element-based analysis of the elastic bending of a simple cantilever beam, of which the exact solution is known. (3) The tetra-04 element-based analysis of the deformation of a wrench. (4) The shell-element-based analysis of a barrel vault. In this paper, we develop a two-step method first to estimate the uncertainty of a converging series of finite-element-mesh-density-parametric solutions using a 4-parameter logistic function, and then to extrapolate the results of a specific quantity (e.g., a stress component) to an extremely fine mesh density approaching the infinite degrees of freedom. The estimated parameter of the upper bound of the logistic function serves as the "best" estimate of the chosen quantity such as a specific stress component. Using a super-parametric approach, as described in Part III of this series, we show that the hexa-27 element is superior to tetra-04, hexa-08, and hexa-20.

Published by Elsevier Ltd. This is an open access article under the CC BY-NC-ND license
(http://creativecommons.org/licenses/by-nc-nd/4.0/).
Peer-review under responsibility of the organizing committee of ICPVT-14

Keywords: ABAQUS; cantilever beam stress analysis; COMSL; Dataplot; element type; finite element method; logistic function; mathematical modeling; mesh density; MPACT; nonlinear least square fit method; parametric method; pipe elbow stress analysis; pressure vessel and piping; super-parametric method; surface crack in piping; TrueGrid; uncertainty quantification; wrench stress analysis

[1] Contribution of the U.S. National Institute of Standards & Technology. Not subject to copyright.

* Corresponding author.
E-mail address: fong2015fong@hotmail.com

1877-7058 Published by Elsevier Ltd. This is an open access article under the CC BY-NC-ND license
(http://creativecommons.org/licenses/by-nc-nd/4.0/).
Peer-review under responsibility of the organizing committee of ICPVT-14
doi:10.1016/j.proeng.2015.12.183

1. Introduction

To quantity the uncertainty of a solution of an industry-based problem using a commercially-available finite element method (FEM) code is extremely challenging, because such problems are generally associated with a complex geometry, a partially-validated material property database, an incomplete knowledge of prior loading histories, and an increasingly user-friendly human-computer interface that provides a quick answer without a standard method of verification and uncertainty estimation. To understand this challenge, one needs to identity, as described in Zienkieuwicz and Taylor [1], Fong, et al. [2]. etc., at least four sources of numerical uncertainties associated with FEM, namely,

(1) Source-1 (Element Type): The choice of a finite element type, such as the tetrahedron element with 4 nodes (tetra-4), hexahedron with 8 nodes (hexa-8), tetrahedron with 10 nodes (tetra-10, with nodes at four corners and six edges), hexahedron with 20 nodes (hexa-20, with nodes at 8 corners and 12 edges), and hexahedron with 27 nodes (hexa-27, with nodes at 8 corners, 12 edges, 6 faces, and the center of the entire hexahedron).

(2) Source-2 (Mesh Density): The change in finite element mesh density (e.g., coarse, normal, fine).

(3) Source-3 (Model Parameters): The variability in geometrical, material property, and boundary condition parameters that are usually bundled together as a single source.

(4) Source-4 (Solution Platform): The choice of a particular finite element analysis code and its solution algorithm, such as ABAQUS [3], ANSYS [4], LS-DYNA [5], MPACT [6], etc.

To address this challenge, we develop a 3-part series of papers, of which this paper is the second part:

Part I (Marcal, Fong, Rainsberger, and Ma [7]): In the first part, we address Source-1 (Element Type) by applying the theory of truncation errors to prove that the 27-node element, Hexa-27, is superior to any of the other commonly-used elements, namely, Tetra-04, Hexa-08, and Hexa-20, because the truncation error of Hexa-27 is h(0)3, and that of the others, h(0)2.

Part II (this paper): In this part, we address Source-2 (Mesh Density) by developing a 2-step method, first to estimate the uncertainty of a converging series of finite-element-mesh-density-parametric solutions of a specific quantity (e.g., a component of stress) using a nonlinear least square fit [8] of a 4-parameter logistic function [9, 10], and then to extrapolate the results of that quantity to an extremely fine mesh density approaching the infinite degrees of freedom. Assuming the chosen quantity increases with mesh density, the estimated upper asymptote of the logistic function serves as the "best" estimate of that chosen quantity. Throughout this paper, we use a public domain statistical analysis software package named "Dataplot" [11] to code the nonlinear least square (NL-LSQ) fit and plot the results.

Part III (Fong, Rainsberger, Marcal, Filliben, Heckert, and Ma [12]): Finally in the third part, we develop a super-parametric method to address not only Source-3 (Model Parameters) by parametrizing the geometry, material properties, and boundary conditions using a FEM pre-processer named TrueGrid [13], but also Source-1, -2, and -4 by parametrizing the element type (Source-1), the mesh density (Source-2), and the solution platform (Source-4).

We begin in this paper by introducing the logistic function in Section 2. We then apply our new approach to three FEM case studies (Sections 3 to 5) to show that it is feasible to extrapolate FEM solutions to an infinite degrees of freedom. For Case 4 on a barrel vault application, see Ref. [7]. Significance and limitations of this approach and concluding remarks are given in Sections 6 and 7, respectfully. A list of references appears at the end of this paper.

2. Logistic Function

A logistic function [8, 9], named after Pierre Francois Verhulst [14] for his use in a study of population growth, is an S-curve with two asymptotes and is commonly represented by the following 4-parameter equation:

$$f(x) = y1 - L / (1 + \exp(-k * (x - a))), \tag{1}$$

here $y1$ is the upper asymptote, $L = y1 - y0$ with $y0$ equal to the lower asymptote, k is the S-curve shape steepness coefficient, and a, the x-value of the S-curve midpoint (sometimes denoted by $x0$).

To visualize this 4-parameter function, let us simplify it by assigning y0=0, and y1=1. Eq. (1) thus becomes a 2-parameter logistic function with two example plots given in Fig. 1. The parameter L is, therefore, a scale factor for the difference between the upper and the lower asymptotes. When L is not unity, and y0 is still zero, we have a 3-parameter logistic function as illustrated by two plots in Fig. 2.

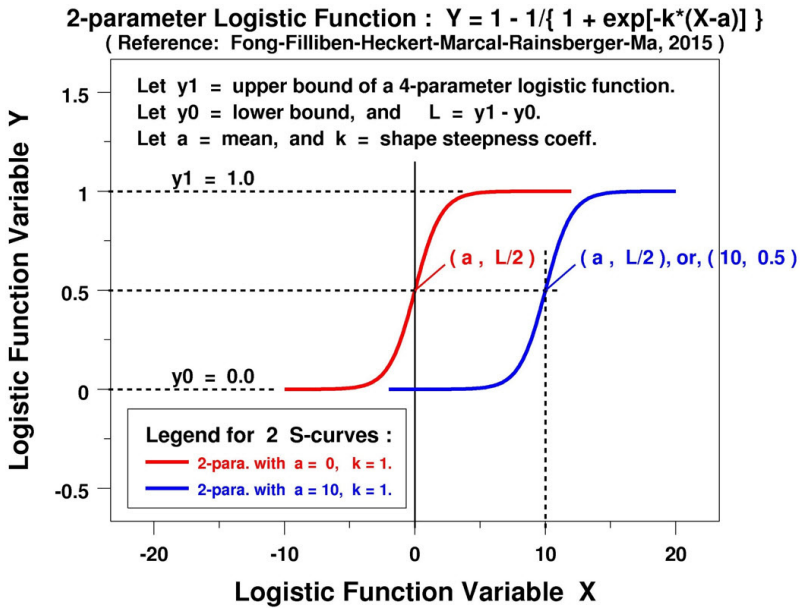

Fig. 1. Plots of Two 2-parameter (*a, k*) Logistic Functions where the two asymptotes are assumed to be 0 (lower) and 1.0 (upper).

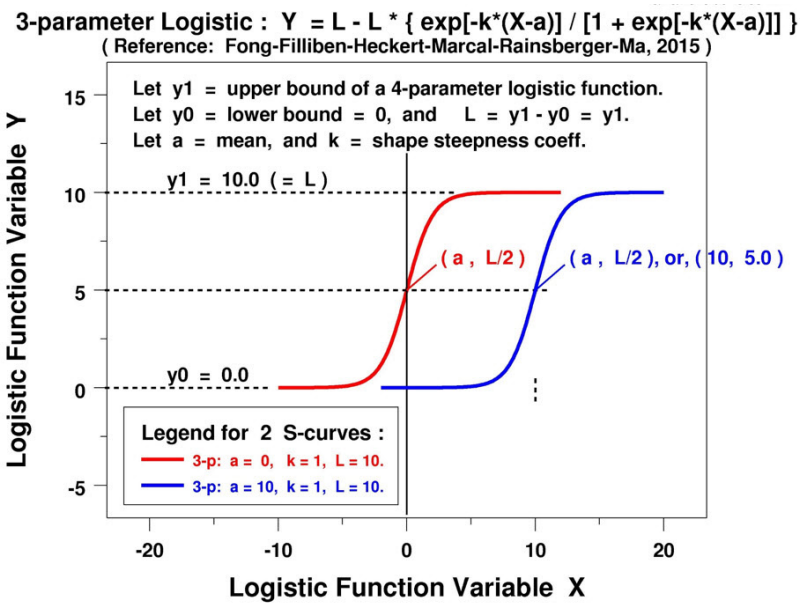

Fig. 2. Plots of Two 3-parameter (*a, k, L*) Logistic Functions, where thelower asymptote is assumed to be zero, and the upper, *L*.

As shown in Refs. [9, 10], an interesting property of f(x) is given by the identity, f(- x) = 1 – f(x). In this paper, we use not only Eq. (1), but also an alternative form (see below) based on that identity:

$$f(x) = y1 - L * (\exp(-k * (x - a) / (1 + \exp(-k * (x - a))))). \quad (2)$$

3. Case 1: A 90-deg Steel Elbow with a Longitudinal Surface Crack in one of its Weldment

In Part 1 of this 3-paper series [7], we showed that FEM simulations with the Hexa-27 element type having truncation errors of h(0)3 , are theoretically more accurate than those with the Hexa-20, Hexa-08, and Tetra-04 element types. This finding addressed our concern for FEM Uncertainty Source-1 (Element Type).

In this paper, which is Part 2 of the 3-paper series, we examine in greater detail how FEM simulations reach their "final" and "credible" answers by constructing a sequence of solutions with increasing mesh densities or degrees of freedom. To address this Uncertainty Source-2 (Mesh Density), we apply a nonlinear least square (NL-LSQ) fit algorithm [8] to any such sequence (minimum 5 points) for a 4-parameter logistic function [9, 10], as defined in Eqs. (1) or (2), such that a predicted solution with uncertainty quantification (UQ) at an infinite degrees of freedom can be rigorously estimated. We describe this unique approach by running three FEM case studies, namely, (1) a 90-deg steel elbow with a longitudinal surface crack, (2) a cantilever beam with an end load, and (3) the stress analysis of a wrench. For the 4th case on a barrel vault application, see Ref. [7].

As shown in Fig. 3, we consider in this section the first case study involving a 900-mm-O.D., 20-mm-thickness, 90-degree elbow welded to two straight pipe sections [15], and a 50-mm-long, 10-mm-deep, 4-mm-wide longitudinal surface crack in one of the two weldments next to the elbow.

We first run a 5-point sequence of Hexa-27 FEM simulations of the elastic deformation of the elbow+crack problem (E = 207 GPa, ν = 0.3) at increasing mesh densities or degrees of freedom using MPACT [6] and a unique FEM-pre-processor code named TrueGrid [13] to compute the Sxx component of the maximum stress at the crack tip due to an application of a horizontal tensile surface distributed load of 50 MPa at one pipe end and a fully fixed boundary condition at the other pipe end (see Fig. 3).

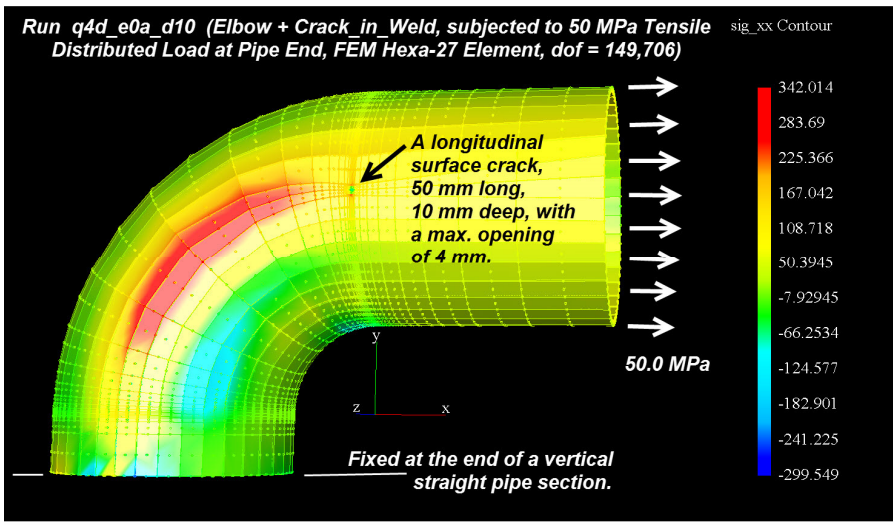

Fig. 3. A finite element solution (MPACT-Hexa-27 at 149,706 deg. of freedom) for the elastic deformation of a pipe-elbow with a longitudinal surface crack in one of its two weldments [7].

The addition of TrueGrid [13] to our FEM simulation toolbox is critical, because it allows us to address all 4 sources of FEM uncertainties defined in Section 1, using a "super-parametric" approach as described in full in the third part [12] of this 3-part series of papers.

In Fig. 4 and Table 1, we present the FEM data and a plot of the NL-LSQ fit of the 5-point sequence of Hexa-27 simulations. Note that the parameter L (= 3.5 MPa) is very small as compared with the value of y1 (= 345.5 MPa), the upper asymptote, indicating that the Hexa-27 does give very accurate results.

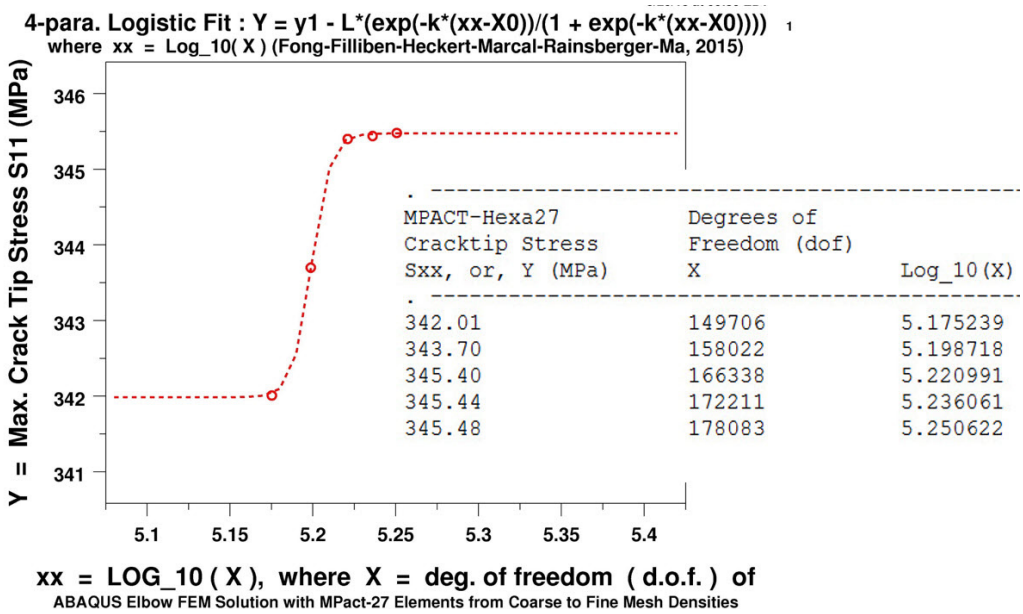

Fig. 4. Plot of a Non-Linear Least Square (NL-LSQ) Fit of 5 MPACT-Hexa-27 Solutions [7].

Table 1. NL-LSQ Fit of 5 MPACT-Hexa-27 Solutions using a 4-para. Logistic Function.

Least Squares Non-Linear Fit for a 4-parameter Logistic Function

Sample Size: 5

Model: Y05 =Y1 - L*(EXP(-K*(XLOG-X0))/(1 + EXP(-K*(XLOG-X0))))

No Replication Case:

Iteration Number	Convergence Measure	Residual Standard Deviation	*	Parameter Estimates			
1	0.1000000E-01	0.1725538E+00	*	0.3454800E+03	0.3500000E+01	0.1778000E+03	0.5200000E+01
2	0.2562891E+00	0.1517191E+00	*	0.3454717E+03	0.3489931E+01	0.1352166E+03	0.5199279E+01
3	0.1281445E+00	0.7402917E-01	*	0.3454715E+03	0.3484673E+01	0.1624932E+03	0.5199241E+01
4	0.2883252E+00	0.6613538E-01	*	0.3454738E+03	0.3485044E+01	0.1759787E+03	0.5199260E+01
5	0.9730975E+00	0.6584587E-01	*	0.3454740E+03	0.3485436E+01	0.1765055E+03	0.5199258E+01
6	0.7298232E+00	0.6583225E-01	*	0.3454741E+03	0.3485567E+01	0.1766631E+03	0.5199258E+01

	Final Parameter Estimates		Approximate Standard Deviation	t-Value
1	Y1	345.4741	0.1739	1987.0615
2	L	3.4856	0.1606	21.7056
3	K	176.6730	70.2464	2.5150
4	X0	5.1993	0.0035	1498.7349

Residual Standard Deviation: 0.0658

Residual Degrees of Freedom: 1

Next, we run a 5-point sequence of Hexa-08 FEM simulations using ABAQUS [3] with results shown in Figs. 5 and 6, and Table 2. It is interesting to see that the upper asymptote, y1 (=221.5 MPa), is only 64 % of that of the MPACT-Hexa-27 runs. In Fig. 7, we add more points to the sequence and learned surprisingly that the upper asymptote, y1 (=231.7 MPa), has only slightly improved to 67 %. Using an algorithm described by Draper and Smith [8], we calculate the predictive limits of the NL-LSQ fit of 11 points, as shown in Fig. 8. To complete our study of this Case 1, we show in Fig. 9 a comparison of FEM solutions using 3 different element types. Note that the upper asymptote of the ABAQUS-Hexa-20 runs, y1 (= 453 MPa), overestimates the more accurate Hexa-27 solution (345.5 MPa) by 31 %.

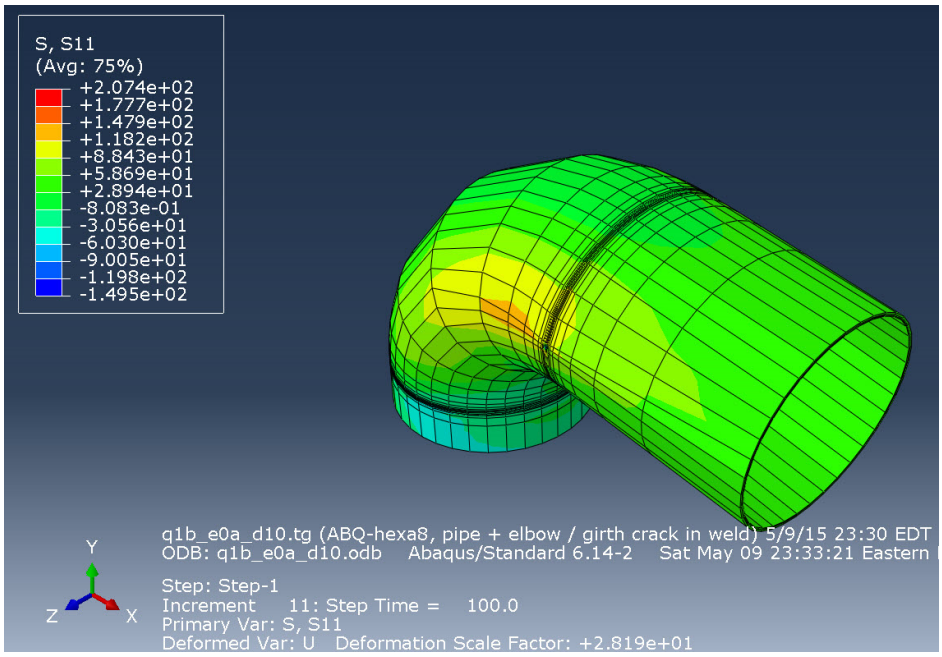

Fig. 5. A finite element solution (ABAQUS-Hexa-08 at 21,069 deg. of freedom) for the elastic deformation of a pipe-elbow with a longitudinal surface crack in one of its two weldments.

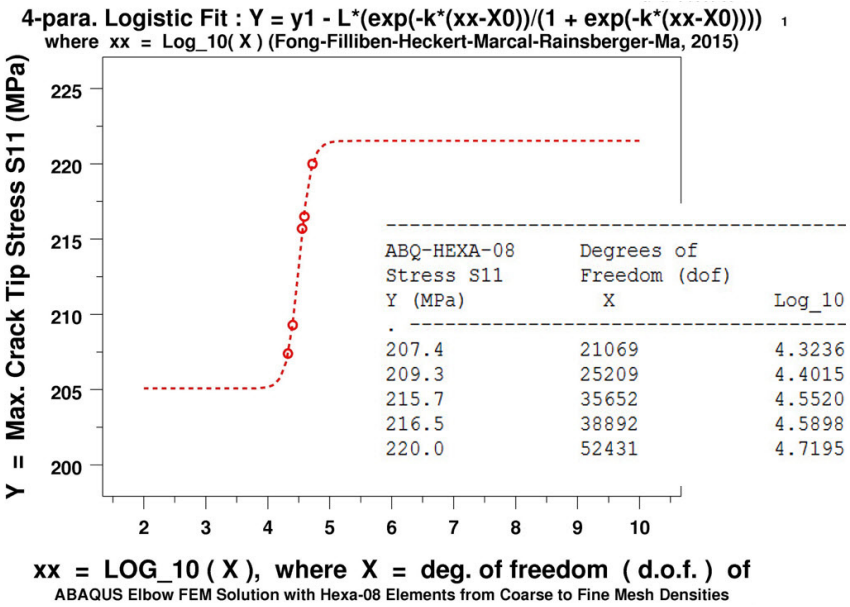

Fig. 6. Plot of a Non-Linear Least Square Fit of 5 ABAQUS-Hexa-08 Solutions.

Table 2. NL-LSQ Fit of 5 ABAQUS-Hexa-08 Solutions using a 4-para. Logistic Function

Least Squares Non-Linear Fit for a 4-parameter Logistic Function

Sample Size: 5

Model: Y05 = Y1 - L*(EXP(-K*(XLOG-X0))/(1 + EXP(-K*(XLOG-X0))))

No Replication Case:

Iteration Number	Convergence Measure	Residual Standard Deviation *	Parameter Estimation Iteration History Y1	L	K	X0
1	0.1000000E-01	0.1020942E+02 *	0.2200000E+03	0.1260000E+02	0.1000000E+01	0.5000000E+01
2	0.5766504E+00	0.9048625E+01 *	0.2210591E+03	0.1186929E+02	0.2238918E+01	0.4505869E+01
3	0.2883252E+00	0.3444835E+01 *	0.2206836E+03	0.1346456E+02	0.9059054E+01	0.4559481E+01
4	0.1441626E+00	0.1020396E+01 *	0.2207778E+03	0.1412043E+02	0.1185153E+02	0.4506715E+01
5	0.7208130E-01	0.4986396E+00 *	0.2209683E+03	0.1503649E+02	0.1185306E+02	0.4507022E+01
6	0.3604065E-01	0.4675306E+00 *	0.2212942E+03	0.1585879E+02	0.1072222E+02	0.4503672E+01
7	0.1802032E-01	0.4498254E+00 *	0.2214899E+03	0.1634952E+02	0.1035461E+02	0.4501993E+01
8	0.9010162E-02	0.4489728E+00 *	0.2215268E+03	0.1643778E+02	0.1030533E+02	0.4501779E+01
9	0.4505081E-02	0.4489694E+00 *	0.2215285E+03	0.1644071E+02	0.1030548E+02	0.4501789E+01

	Final Parameter Estimates	Approximate Standard Deviation	t-Value
1 Y1	221.5286	1.4380	154.0572
2 L	16.4409	3.5706	4.6045
3 K	10.3052	3.6430	2.8287
4 X0	4.5018	0.0278	162.2190

Residual Standard Deviation: 0.4490

Residual Degrees of Freedom: 1

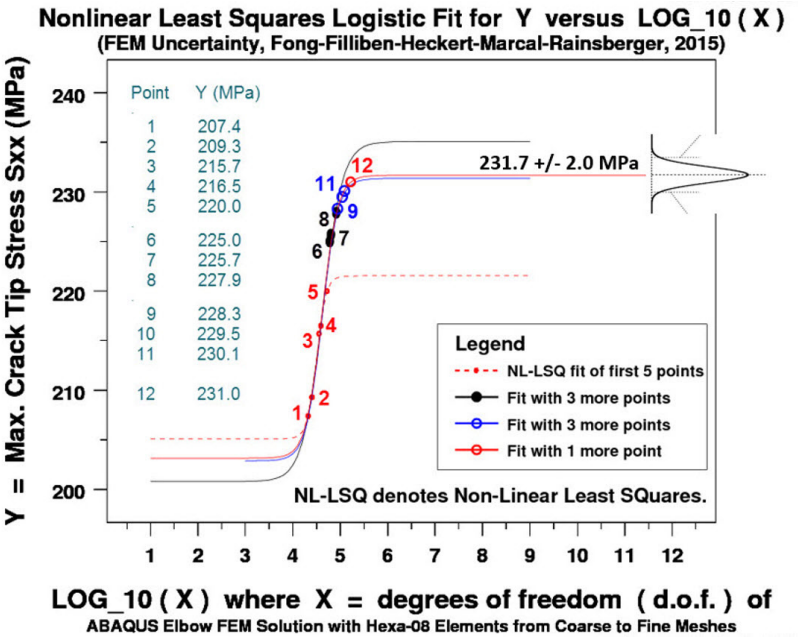

Fig. 7. Plots of Non-Linear Least Square Fits of 4 sets of ABAQUS-Hexa-08 Solutions of Max. S_{xx} using a total of 12 points: (1) 1 to 5, (2) 1 to 8, (3) 1 to 11, and (4) 1 to 12.

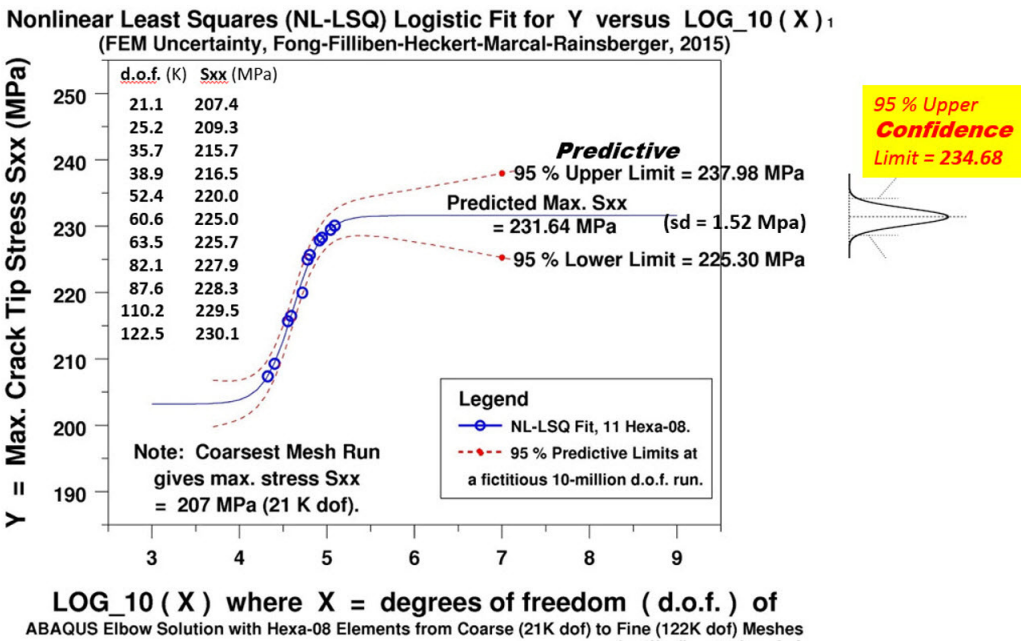

Fig. 8. Plot of a NL-LSQ Fit of 11 ABAQUS-Hexa-08 Solutions with Predictive Limits.

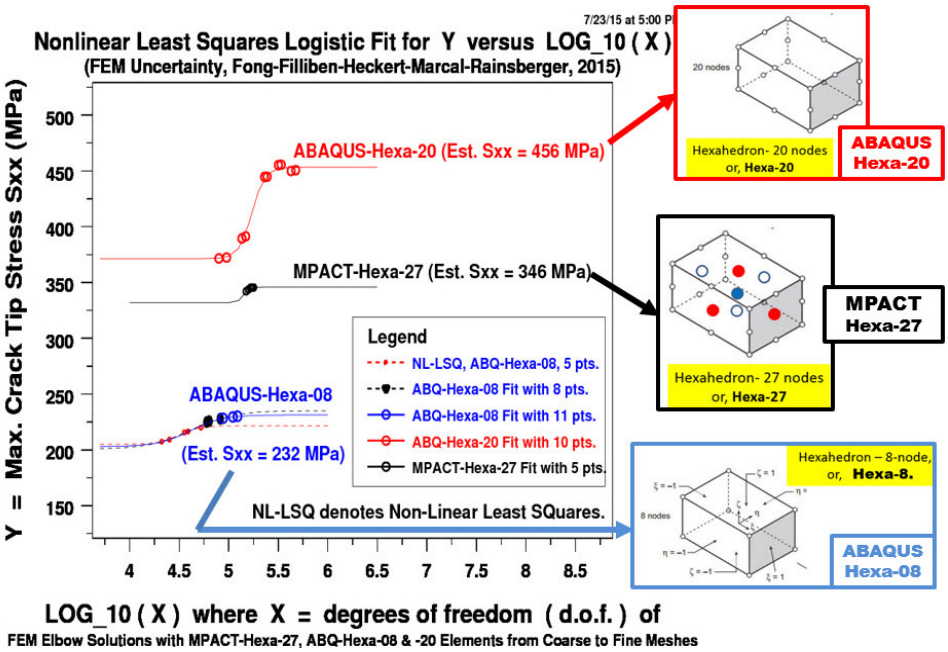

Fig. 9. A Comparison of FEM Elbow+Crack Solutions using 3 element types with details of 10 ABAQUS-Hexa-20 solutions with NL-LSQ fit results in two inserts.

4. Case 2. Elastic Bending of a Horizontal Cantilever Beam under a Vertical End Load

To validate our new approach of estimating an FEM simulation result at infinite degrees of freedom using a logistic nonlinear least square (NL-LSQ) fit (Section 3) and a super-parametric FEM algorithm written in TrueGrid [12, 13], we introduce an elementary problem in classical structural mechanics, of which we know its theoretical solution in a set of simple formulas. That problem is the elastic deformation of a simple cantilever beam with an end load (see, e.g., Hool and Johnson [16]).

As shown in Fig. 10, we choose to work with a simple cantilever beam, 100-mm long, 10-mm wide, and 2-mm thick, with the left end of a horizontal beam fixed and the right end loaded vertically by a force of 1 N. Assuming a Young's modulus of 200 GPa and a Poisson's ratio of 0.3, the theoretical solution of this simple problem [16] yields two interesting answers, namely, the maximum bending stress at the fixed end is 15.0 MPa, and the deflection at the right end is -0.25 mm.

Since the problem is linear, and the maximum bending stress is directly proportional to the applied load, we choose to work with a much higher load, say, 100 N., instead of 1.0 N., even though the deflection will be too high for the linearity assumption to hold. Our numerical results in the estimated maximum bending stress, as displayed in Figs. 10-12 and Table 3, need to be divided by 100 in order for the assumption of linearity to hold. Nevertheless, this scaling up by a factor of 100 does not alter the validity of our investigation in Case 2, where the maximum bending stress will be known to be 1,500 MPa.

Since the problem is linear, and the maximum bending stress is directly proportional to the applied load, we choose to work with a much higher load, say, 100 N., instead of 1.0 N., even though the deflection will be too high for the linearity assumption to hold. Our numerical results in the estimated maximum bending stress, as displayed in Figs. 10-12 and Table 3, need to be divided by 100 in order for the assumption of linearity to hold. Nevertheless, this scaling up by a factor of 100 does not alter the validity of our investigation in Case 2, where the maximum bending stress will be known to be 1,500 MPa.

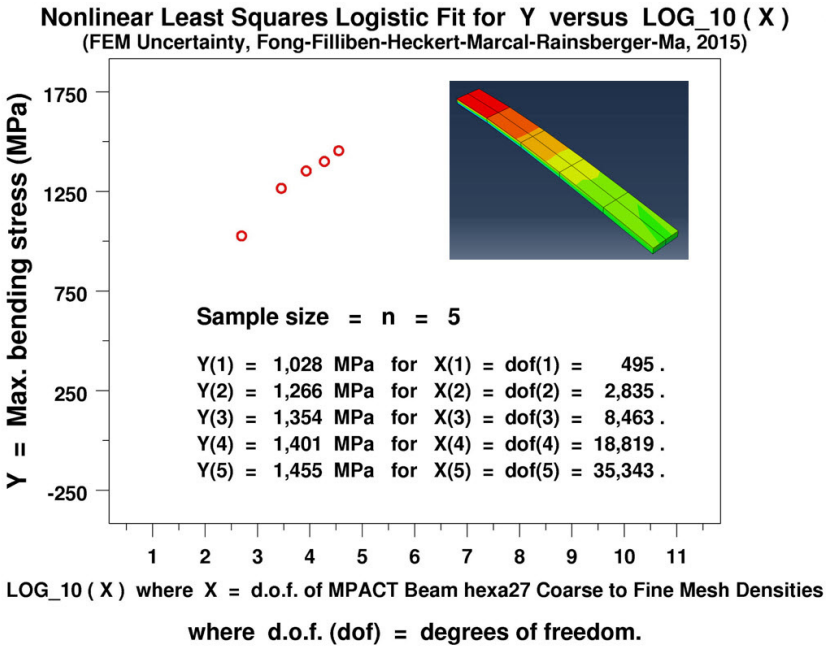

Fig. 10. Plot of 5 MPACT-Hexa-27 solutions of the max. bending stress in a horizontal Isotropic elastic cantilever beam with a vertical load at its free end.

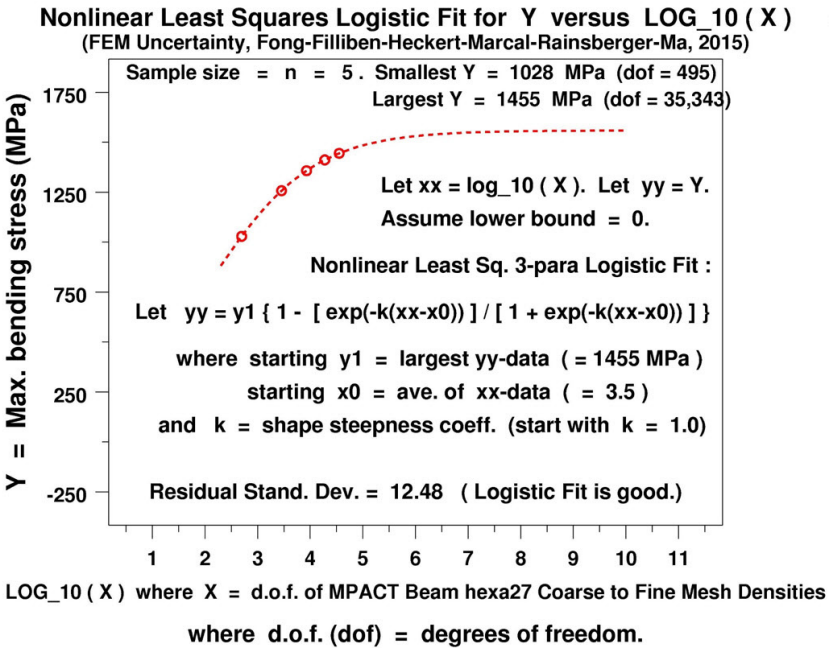

Fig. 11. Plot of a NL-LSQ Fit of 5 MPACT-Hexa-27 solutions of max. bending stress.

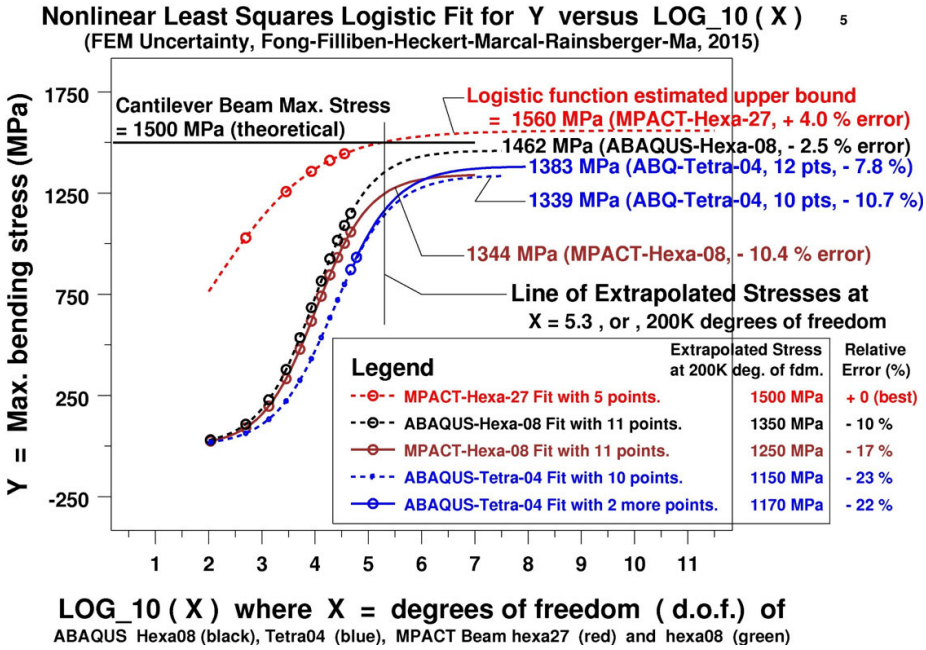

Fig. 12. A Comparison of FEM Simple Cantilever Beam Solutions using MPACT-Hexa-27, MPACT-Hexa-08, ABAQUS-Hexa-08, and ABAQUS-Tetra-04 element types and NL-LSQ Fits.

Table 3. NL-LSQ Fit of 5 MPACT-Hexa-27 Solutions Using a 3-para. Logistic Function.

```
            Least Squares Non-Linear Fit

Sample Size:                                        5

Model: Y05 =Y1 * (1 - EXP(-K*(XLOG-X0))/(1 + EXP(-K*(XLOG-X0))))

No Replication Case:
```

Iteration Number	Convergence Measure	Residual Standard Deviation *	Parameter Estimates Y1	K	X0
1	0.1000000E-01	0.7661341E+03 *	0.1455190E+04	0.1000000E+01	0.3500000E+01
2	0.5000000E-02	0.3048972E+03 *	0.1871536E+04	0.3285880E+00	0.2577974E+01
3	0.1687500E-01	0.1961384E+03 *	0.1361897E+04	0.6511781E+00	0.3973272E+00
4	0.1922168E+00	0.1907965E+03 *	0.1573409E+04	0.7577947E+00	0.2247790E+01
5	0.9610840E-01	0.1621298E+02 *	0.1615401E+04	0.8456184E+00	0.1998429E+01
6	0.4805420E-01	0.1386572E+02 *	0.1597001E+04	0.9040343E+00	0.2025783E+01
7	0.2402710E-01	0.1280894E+02 *	0.1569081E+04	0.9749697E+00	0.2029749E+01
8	0.1201355E-01	0.1248537E+02 *	0.1560926E+04	0.1005668E+01	0.2036577E+01
9	0.6006775E-02	0.1248091E+02 *	0.1559952E+04	0.1009492E+01	0.2037321E+01

	Final Parameter Estimates		Approximate Standard Deviation	t-Value
1	Y1	1559.9074	49.7004	31.3862
2	K	1.0096	0.1554	6.4970
3	X0	2.0373	0.0572	35.6205

```
Residual Standard Deviation:            12.4809
Residual Degrees of Freedom:            2
```

In Fig. 10, using the MPACT-Hexa-27 element and a super-parametric algorithm written in TrueGrid [12, 13], we show the results of a 5-point FEM simulations for degrees of freedom ranging from 495 to 35,343. The maximum bending stress for those five mesh densities varies from a low of 1,028 MPa to a high of 1,455 MPa, the latter of which differs from the theoretical solution (1,500 MPa) by only – 3 %.

In Fig. 11 and Table 3, we show the results of a 3-parameter logistic NL-LSQ fit (assuming the lower asymptote to be zero to simplify computation). The upper asymptote, y1 , is found to be 1,560 MPa, which differs from the theoretical solution by + 4 %. The standard deviation (s.d.) of y1 is 50 MPa, so it is reasonable to estimate the 95 % confidence interval of the maximum bending stress at 2*s.d. to be (1,460, 1,660 MPa), which certainly contains the theoretical solution (= 1,500 MPa).

In Fig. 12, we show the results of four FEM simulations using not only the MPACT-Hexa-27 as shown in Figs. 10-11, but also MPACT-Hexa-08, ABAQUS-Hexa-08, and ABAQUS-Tetra-04. The results of extrapolating to 200K and infinite degrees of freedom again show the superiority of the Hexa-27 element as documented in Part 1 of this 3-paper series [7]. For example, when we extrapolate all the FEM simulation results to 200K degrees of freedom (see table at lower right of Fig. 12), the MPACT-Hexa-27 element shows zero error, where the other element types show errors ranging from -10 to -23 %. When we extrapolate the results to the infinite degrees of freedom (see data on the upper right of Fig. 12), the MPACT-Hexa-27 shows an error of +4 %, where the others show errors ranging from -2.5 to -10.7 %.

5. Case 3: Stress Analysis of a Wrench

In engineering offices around the world, commercially-available FEM-based software packages are a mainstay of an engineer' toolbox. The most popular element type is the Tetra-04 element, because there exists an automatic mesh generator in each of those commercially-available FEM packages. An example of this is found in a package named COMSOL [16], where an example problem on the stress analysis of a wrench using a parametric method on its mesh densities is included.

In a paper by Fong, et al. [17], we examine the uncertainty quantification of the FEM simulations of that COMSOL wrench problem in great detail using our new approach. The results of our investigation are given in Figs. 13-14 and Table 4.

In Fig. 13, we display a 5-point sequence of COMSOL-Tetra-04 simulations for degrees of freedom ranging from 10,743 (coarse) to 123,657 (fine). The maximum Mises stress varies from 322.45 MPa to 364.35 MPa, with an upper asymptote prediction of 366,34 MPa based on Table 4. Since the 4th point of the 5-point sequence predicts a stress of 355.02 MPa, or, about -2.5 % from the 5th point value (364.35), we need to add more simulation points to reach at least a +1 or -1 % variation.

As shown in Fig. 14, we continue to refine the mesh density to improve the result. As we reach the 8th and 9th points, the predicted Mises stress varies from 369.24 (d.o.f. = 732,220) to 369.72 MPa (d.o.f. = 1,119,600), a fact that we have reached the +1 or -1 % criterion. Using our 4-parameter logistic NL-LSQ fit approach, we obtain an upper asymptote value of 369.2 MPa with a s.d. of 0.6 MPa. To validate this result, we run a COMSOL-Tetra-04 simulation to a very fine mesh density (d.o.f. = 6,932,883), with a max. Mises stress of 369.71 MPa, which lies comfortably within the predicted 95 % confidence level.

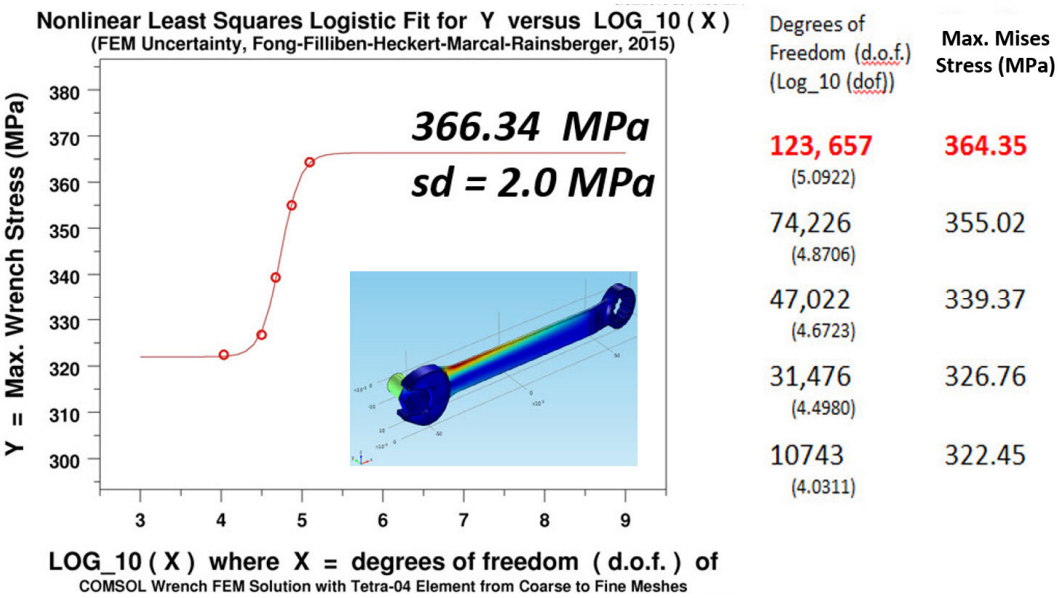

Fig. 13. A NL-LSQ Fit of 5 COMSOL-Tetra-04 Solutions of Max. Mises Stress in a Wrench.

Table 4. NL-LSQ Fit of 5 COMSOL-Tetra-04 Solutions using a 4-para. Logistic Function.

A Non-Linear Least Square Fit using an S-curve Logistic Function:

```
Least Squares Non-Linear Fit for:        COMSOL Wrench Stress Analysis (5 Fine to Coarse Meshes)

4-Parameter Logistic Function Model:     YO5 = Y1 - L*(EXP(-K*(XLOG-XO))/(1 + EXP(-K*(XLOG-XO))))

Sample Size:    5                        No Replication Case:
```

Iteration Number	Convergence Measure	Residual Standard Deviation *	Parameter Estimates			
1	0.1000000E-01	0.2886132E+02 *	0.3643500E+03	0.4190000E+02	0.1000000E+01	0.5000000E+01
2	0.1139062E+00	0.2782295E+02 *	0.3720484E+03	0.3211696E+02	0.4972718E+01	0.4835044E+01
3	0.5695313E-01	0.1013394E+02 *	0.3644373E+03	0.4212619E+02	0.8006263E+01	0.4635532E+01
4	0.2847656E-01	0.1516070E+01 *	0.3659203E+03	0.4371380E+02	0.8126122E+01	0.4737073E+01
5	0.1423828E-01	0.1218623E+01 *	0.3663495E+03	0.4436871E+02	0.8229342E+01	0.4733777E+01
6	0.7119141E-02	0.1217993E+01 *	0.3663420E+03	0.4436198E+02	0.8250083E+01	0.4733750E+01
7	0.3559570E-02	0.1217981E+01 *	0.3663429E+03	0.4436449E+02	0.8248517E+01	0.4733739E+01

	Final Parameter Estimates		Approximate Standard Deviation	t-Value
1	Y1	366.3426	2.0070	182.5263
2	L	44.3641	2.5945	17.0992
3	K	8.2487	1.0702	7.7076
4	XO	4.7336	0.0194	243.7687

366.34 MPa
s.d. = 2.0 MPa

```
Residual Standard Deviation:                    1.2179
Residual Degrees of Freedom:                         1
```

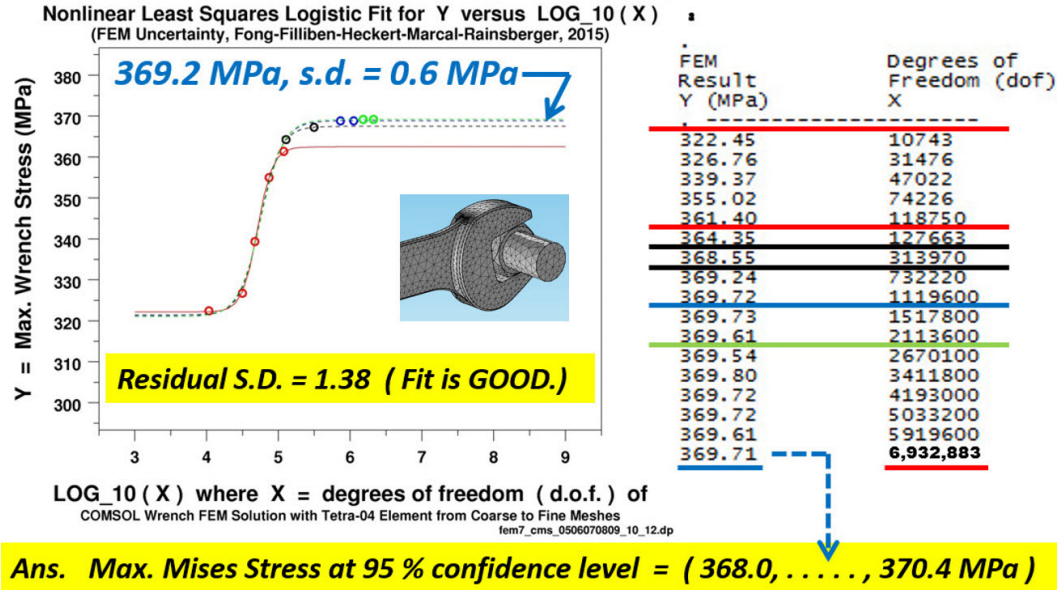

Fig. 14. A Comparison of the predicted max. Mises stress with uncertainty estimate from a NL-LSQ Fit of 11 COMSOL-Tetra-04 solutions with a validation run at 7 million deg. of freedom.

6. Significance and Limitations

By addressing in this paper the uncertainty source-2 (mesh density) using a 4-parameter logistic nonlinear least square fit approach, we present a rigorous method of finding the so-called "best" FEM solution corresponding to the infinite degrees of freedom.

As discussed in the other two companion papers [7, 12], the approach described in this paper needs to be combined with the super-parametric approach [12] in order to arrive at the "best" possible solution with uncertainty quantification. What is significant about the logistic NL-LSQ fit approach is the fact that, for the first time in the history of the development of the FEM method, one now has a tool to extrapolate, with confidence, a sequence of simulations at increasing mesh densities beyond the memory and speed limitations of a laptop computer.

For engineering problems with complex geometry and hard-to-characterize material properties and boundary conditions, this new approach is not without limitations, namely, the uncertainty of the FEM simulations still depends on the uncertainties of the model parameters. To address that dependence, we need a different tool, namely, the statistical design of experiments (see Fong, et al. [18]).

7. Concluding Remarks

By presenting the numerical results of 3 case studies, we show in this paper that a new approach of fitting a sequence of FEM simulations at increasing mesh densities is feasible in obtaining the "best" solution by extrapolating to the infinite degrees of freedom. This new fitting approach is rigorous in the sense it uses a 4-parameter logistic function and a nonlinear least square fitting algorithm. We have also shown, through the presentation of the results of 3 case studies, that when we combine this NL-LSQ fitting approach with a super-parametric FEM coding technique (see Part 3 [12] of the 3-part series), we can address the FEM uncertainties due to all four sources, namely, the element type, the mesh density, the model parameters, and the solution platform.

8. Disclaimer

Certain commercial equipment, instruments, materials, or computer software is identified in this paper in order to specify the experimental or computational procedure adequately. Such identification is not intended to imply recommendation or endorsement by the National Institute of Standards and Technology, nor is it intended to imply that the materials, equipment, or software identified are necessarily the best available for the purpose.

References

[1] O.C. Zienkiewicz, R.L. Taylor, The Finite Element Method, fifth ed., Vol. 1: The Basis, Sections 8.3 and 8.4, pp. 168-172. Butterworth-Heinemann, 2000.

[2] J.T. Fong, J.J. Filliben, N.A. Heckert, R. deWit, Design of Experiments Approach to Verification and Uncertainty Estimation of Simulations based on Finite Element Method, Proc. Conf. Amer. Soc. For Eng. Education, June 22-25, Pittsburgh, PA, AC2008-2725, 2008.

[3] Anon., Abaqus/CAE User's Guide, and Abaqus Analysis User's Guide, version 6.13. Dassault Systemes Simulia Corp., Providence, RI, U.S.A. , 2015, http://www.3ds.com/products-services/simulia/support/documentation/

[4] Anon., Ansys Multiphysics User's Manual, Release 16.0. ANSYS, Inc., Canonsburg, PA, U.S.A., http://www.ansys.com/Support/Documentation, 2015.

[5] Anon., LS-DYNA R8.0 Keyword Manual Vols. I, II, and III. Livermore Software Technology Corp., 7374 Las Positas Road, Livermore, CA 94551, U.S.A., http://www.lstc.com/, 2015

[6] P.V. Marcal, MPACT User Manual, Mpact Corp. , Oak Park, CA, 2001.

[7] P.V. Marcal, J.T. Fong, R. Rainsberger, L. Ma, Finite Element Analysis of a Pipe Elbow Weldment Creep- Fracture Problem Using an Extremely Accurate 27-node Tri-Quadratic Shell and Solid Element Formulation, Proc. 14th International Conf. on Pressure Vessel Technology, ICPVT-14, Sep. 23-26, 2015, Shanghai, China, 2015.

[8] N.R. Draper, H. Smith, Applied Regression Analysis, Chapters 1-3, pp. 1-103, and Chapter 10, pp. 263-304. Wiley , 1966.

[9] M. Evans, N. Hastings, B. Peacock, Statistical Distributions, third ed., pp. 124-128. Wiley , 2000.

[10] N. Balakrishnan, Handbook of the Logistic Distribution. Marcel Dekker, New York , 1992.

[11] J.J. Filliben, N.A. Heckert, Dataplot: A Statistical Data Analysis Software System, National Institute of Standards & Technology, Gaithersburg, MD 20899 , 2002, http://www.itl.nist.gov/div898/software/dataplot.html

[12] J.T. Fong, R. Rainsberger, P.V. Marcal, J.J. Filliben, N.A. Heckert, L. Ma, A Super-Parametric Approach to Assessing the Accuracy of Finite Element Method-estimated Results by Increasing Mesh Density and Varying Element Types using ABAQUS and MPACT, Proc. International Conf. on Pressure Vessel Technology, ICPVT-14, Sep. 23-26, 2015, Shanghai, China, 2015.

[13] R. Rainsberger, TrueGrid User's Manual: A Guide and a Reference, Volumes I, II, and III, Version 3.0.0. Published by XYZ Scientific Applications, Inc., Pleasant Hill, CA 94523 , 2014, www.truegrid.com/pub/TGMAN300.1.pdf.

[14] P.F. Verhulst, Recherches mathematiques sur la loi d'accroissement de la population [Mathematical Researches into the Law of Population Growth Increase], 1845, re-published in Nouveaux Memoires de l'Academie Royale des Sciences et Belles-Lettres de Bruxelles, Vol. 18, pp. 1-42 , 2013.

[15] Anon., Engineering Data, p.43. Joliet, IL 60431: Crane Valves , 1994.

[16] G.A. Hool, N.C. Johnson, Handbook of Building Construction: Data for Architects, Designing and Constructing Engineers, and Contractors, first ed. McGraw-Hill , 1920.

[17] Anon., Introduction to COMSOL Multiphysics, version 5.1. Burlington, MA: COMSOL, Inc., http://cdn.comsol.com/documentation/5.1.0.180/IntroductionToCOMSOLMultiphysics.pdf , 2015.

[18] J.T. Fong, J.J. Filliben, N.A. Heckert, L. Ma, Uncertainty of Finite Element Method-based Solutions Using a Nonlinear Least Square Fit and Design of Experiments Approach, to appear in Proc. Annual COMSOL International User's Conference, Oct. 7-9, 2015, Boston, MA, http://www.comsol.com/conference2015/ , 2015.